

# Lawrence Berkeley National Laboratory

## Recent Work

### Title

SINTERING UNDER LOW APPLIED STRESS: CdO

### Permalink

<https://escholarship.org/uc/item/0w98p4ct>

### Authors

Rahaman, M.N.  
Jonghe, L.C. De

### Publication Date

1984-07-01

LBL-18049

c.2

LBL-18049  
Preprint

RECEIVED  
LAWRENCE  
BERKELEY LABORATORY

SEP 10 1984

LIBRARY AND  
DOCUMENTS SECTION

Submitted to the Journal of  
the American Ceramic Society

SINTERING UNDER LOW APPLIED  
STRESS: CdO

M.N. Rahaman and L.C. De Jonghe

July 1984

**CCAM**

**TWO-WEEK LOAN COPY**

*This is a Library Circulating Copy  
which may be borrowed for two weeks.*

Lawrence Berkeley Laboratory  
University of California  
Berkeley, California 94720

Prepared for the U.S. Department of Energy  
under Contract DE-AC03-76SF00098

**Center  
for  
Advanced  
Materials**

LBL-18049  
c.2

## **DISCLAIMER**

This document was prepared as an account of work sponsored by the United States Government. While this document is believed to contain correct information, neither the United States Government nor any agency thereof, nor the Regents of the University of California, nor any of their employees, makes any warranty, express or implied, or assumes any legal responsibility for the accuracy, completeness, or usefulness of any information, apparatus, product, or process disclosed, or represents that its use would not infringe privately owned rights. Reference herein to any specific commercial product, process, or service by its trade name, trademark, manufacturer, or otherwise, does not necessarily constitute or imply its endorsement, recommendation, or favoring by the United States Government or any agency thereof, or the Regents of the University of California. The views and opinions of authors expressed herein do not necessarily state or reflect those of the United States Government or any agency thereof or the Regents of the University of California.

## SINTERING UNDER LOW APPLIED STRESS: CdO

M. N. Rahaman\* and L. C. De Jonghe\*

Center for Advanced Materials  
Lawrence Berkeley Laboratory  
and  
Department of Materials Science and Mineral Engineering  
University of California  
Berkeley, California 94720

### ABSTRACT

A loading dilatometer of novel design has been used to study the sintering behaviour of CdO powder compacts subjected to low stresses between 0 and 0.25 MPa and at temperatures between 973 and 1123K. Densification and creep occur simultaneously. While both the volumetric densification rate and the uniaxial creep rate show an approximately inverse relation with time, their dependence on stress is markedly different. The uniaxial creep rate increases with stress but the volumetric densification rate is independent of stress.

---

\* Member, American Ceramic Society.

This work was supported by the Division of Materials Science, Office of Basic Energy Services, U. S. Department of Energy, under Contract No. DE-AC03-76SF00098.

## INTRODUCTION

A major problem in the processing of ceramics, and one that is currently receiving much attention, concerns inhomogeneities<sup>1,2,3</sup> in the green body. These inhomogeneities, such as agglomerates and spacial density variations, give rise to differential sintering rates and stresses within the compact during densification, and may lead to the development of crack-like voids in the sintered body. The calculation of these stresses at a microscopic level is extremely difficult, so the problem is being addressed experimentally on a macroscopic level. In a recent study,<sup>4</sup> a higher-density compact of  $\text{Al}_2\text{O}_3$  - 30%  $\text{ZrO}_2$  was forced to shrink uniaxially at the same rate as a lower-density compact at temperatures between 1173 and 1873K by application of a measured applied stress. No attempt was made to separate the shrinkage due to creep from that due to densification in the higher-density compact subjected to the applied stresses.

The approach of the present authors is to use a newly developed loading dilatometer to study the differential sintering of two powder compacts, one undergoing sintering under no stress and the other subjected to a small uniaxial stress. This paper presents the initial results of our work, emphasizing the usefulness of the methods, and deals with the sintering of CdO powder compacts subjected to low, uniaxial stresses between 0 and 0.25 MPa at temperatures between 973 and 1123K. CdO was used because it sinters to relatively high densities within the temperature range suitable for the apparatus. One

advantage of the unconstrained sintering method described here is that inaccuracies due to die-wall friction, as in hot-pressing at low stresses, do not occur. Some friction exist at the contact areas, but since strains remain low, the effect is not dominant.

## EXPERIMENTAL PROCEDURE

CdO powder\* was uniaxially pressed at 20 MPa into cylindrical compacts (6mm by 6mm), and then isostatically pressed at 68 MPa. Compacts with a green density  $0.58 \pm 0.01$  of the theoretical density were sintered in flowing air ( $50 \text{ cm}^3/\text{min}$  for two hours in the loading dilatometer.

A sketch of the loading dilatometer is shown in Fig. 1. The instrument is described in detail elsewhere.<sup>5</sup> The load on one compact was supplied by compressed  $\text{N}_2$  gas acting against a piston and was monitored with a digital strain indicator using a strain gauge\*\* attached to the piston. The load can be applied and removed quickly (<5 seconds) by opening and closing appropriate pin-head valves. In these experiments, the second compact, subjected to no load, was a quartz cylinder (8mm diameter by 6mm). Continuous measurement of the axial shrinkage was made using two quartz push rods (6.5 mm diameter), a sensitive transducer\*\* and an amplifier.\*\*

---

\* Reagent Grade, J. T. Baker Chemical Co., Phillipsburg, N. J. 08865.

\*\* Engineering and Technical Services, Lawrence Berkeley Laboratory, Berkeley, CA 94720.

+ Model V/E-20A, Measurements Group, Raleigh, N. C.

++ Model 300C/60, Daytronic Corporation, Dayton, O. H.

For the experiments, the CdO compact and the quartz pellet were placed in position. After the furnace had reached the working temperature, the sample was introduced quickly into the hot zone. The load on the CdO compact was applied rapidly, and the axial shrinkage and temperature recorded. The mass and dimensions of the compacts were measured before and after sintering and the final density measured, using Archimedes' Principle.

In a separate set of experiments, sintering was terminated after times between 0 and 2 hours. The dimensions of these compacts were measured using a micrometer and the fracture surfaces and polished surfaces examined using scanning electron microscopy.

Experiments in which the load was changed during sintering, were also performed. In these, compacts were sintered under constant load to a certain relative density ( $\rho \sim 0.8$ ) and then the load was quickly changed.

## RESULTS

Figure 2 shows results for the axial shrinkage,  $\Delta L/L_0$  versus time,  $t$ , at two temperatures 973K and 1123K, and for different applied loads between 0 and 0.5 kg ( $L_0$  = initial sample length;  $\Delta L = L - L_0$ , where  $L$  = instantaneous sample length). A load of 0.1 kg represents a stress of 45 kPa and  $t = 0$  represents the commencement of shrinkage. The sintering temperature was reached after a time  $t = 6$  min at 973K and  $t = 8$  min at 1123K. Each curve is the average of two runs under the same conditions. Previous experiments showed that the curves were reproducible to within  $\pm 2\%$ . Weight losses in the sintered pellets were

~ 0.7% after 2 hours, and the applied loads could be maintained to within  $\pm 5\%$ . The shrinkage and the effect of load are small at 973K. The remaining results will be for the temperature of 1123K only.

The application of load causes anisotropic shrinkage of the compact. This is shown in Fig. 3 where the axial shrinkage,  $\Delta L/L_0$  is plotted versus the radial shrinkage,  $\Delta D/D_0$ , between  $t \sim 10$  and  $t = 120$  minutes ( $D_0$  = initial sample diameter;  $\Delta D = D - D_0$ , where  $D$  = instantaneous sample diameter).  $\Delta L/L_0$  is approximately proportional to  $\Delta D/D_0$  and the slopes of the lines increase with increasing load.

A methodology described by Raj,<sup>6</sup> and Figures 2 and 3 were used to separate the creep strain,  $\epsilon$ , from the strain due to densification. Figures, 4 and 5 show the results for  $\epsilon$  versus  $\log t$  and the relative density,  $\rho$ , versus  $\log t$ , respectively. Between  $t \sim 10$  and  $\sim 120$  minutes both  $\epsilon$  and  $\rho$  vary approximately linearly with  $\log t$ . However, at any time in this range,  $\epsilon$  increases with load but  $\rho$  is independent of load. After two hours the relative density,  $\rho$ , is about 0.9, in good agreement with the value determined by using Archimedes' Principle.

Figure 6 shows the results for  $d\epsilon/dt$  and  $d\rho/dt$  versus the applied stress,  $\sigma$ , for  $\rho$  between 0.78 and 0.88.  $d\epsilon/dt$  increases linearly with  $\sigma$  but  $d\rho/dt$  is independent of  $\sigma$ . The non-zero value of  $d\epsilon/dt$  at  $\sigma=0$  may be due to the low tension springs attached to the transducer system that keep the compacts in position.

Figure 7 shows a scanning electron micrograph of a polished section of a compact sintered to  $\rho = 0.88$ . The porosity has mostly agglomerated at the grain corners but there is still some along the



grain boundaries.

The response of the compacts to a change in load during the sintering experiment is shown in Fig. 8. The axial shrinkage rate  $d(\Delta L/L_0)/dt$  is plotted versus  $t$ , for two experiments, one in which the load was increased from 0 to 0.5kg at  $t = 20$  min. (Curve A), and the other in which the load was decreased from 0.5 to 0 kg at  $t = 24$  min. (Curve B). For comparison, the axial shrinkage rates for experiments under constant loads of 0 and 0.5 kg are also shown (Curves C and D, respectively). Two features are of interest. First, after the change in load, curves A and D and Curves B and C do not coincide. Second, for about one minute after the change in load, the shrinkage rates change rapidly before settling down to a smooth variation with time. As illustrated, curve B decrease rapidly then increases again. This second feature is not due to a mechanical instability in the instrument since experiments under the same conditions but using a hot-pressed silicon nitride specimen showed that the readings of load and shrinkage stabilized to constant values within 5 seconds after the change in load.

## DISCUSSION

It is clear that there are two processes occurring, densification and constant volume creep, during the sintering of CdO subjected to the low loads used in these experiments. The somewhat similar dependence of  $d\epsilon/dt$  and  $d\rho/dt$  on  $t$  does not necessarily mean that the two processes are interdependent. The linear dependence of  $d\epsilon/dt$  on  $\rho$  appears to rule out dislocation processes for creep mechanism. Rather,

the applied stresses are small compared to those generated by the surface tension and curvature, so that deformation is likely to be accommodated by the same transport mechanisms that are active in unstressed densification, combined with possible grainboundary sliding due to the shear component of the applied stress.

A most interesting feature of these results, however, is seen in figure 6 where  $d\epsilon/dt$  increases markedly with  $\epsilon$  but  $d\rho/dt$  is independent of  $\epsilon$ . For the three densities shown,  $d\epsilon/dt$  increases about four times between 0.05 and 0.2 MPa but there is no change in the volumetric densification rate,  $d\rho/dt$ .

The application of load during sintering causes a bias in the direction of material movement and possible grainboundary sliding, leading to anisotropic shrinkage of the compact. This can account for the difference between curves A and D and B and C after the change in load (Fig. 8). Furthermore, the nature of the changes in the axial shrinkage rate following the change in the load strongly suggests that storage of anelastic strain energy occurs in the compact. Such stored anelastic strain can, e.g., arise from a pore shape bias introduced as the result of the constant volume deformation.

The method used in this work makes more variables accessible for sintering studies. The application of small loads and load changes to a sintering compact has produced results that cannot be adequately interpreted in terms of simple, two-sphere sintering models.

## REFERENCES

1. A. G. Evans, "Considerations of Inhomogeneity Effects in Sintering," J. Amer. Ceram. Soc., 65 [10] 497 (1982).
2. F. F. Lange, "Sinterability of Agglomerated Powders," J. Amer. Ceram. Soc., 67 [2] 83 (1984)
3. W. H. Rhodes, "Agglomerate and Particle Size Effects on Sintering Yttria-Stabilized Zirconia," J. Amer. Ceram. Soc., 64 [1] 19 (1981)
4. B. Kellet and F. F. Lange, "Stresses Induced by Differential Sintering in Powder Compacts," J. Amer. Ceram. soc., 67 [5] 369 (1984).
5. M. N. Rahaman and L. C. De Jonghe, "A Loading Dilatometer", submitted to Rev. Sci. Instr., (1984).
6. R. Raj, "Separation of Cavitation - Strain and Creep - Strain During Deformation," J. Amer. Ceram. Soc., 65 [3] C-46 (1982)

## LIST OF FIGURES

- Figure 1. Schematic diagram of the loading dilatometer.
- Figure 2. Axial shrinkage versus time for CdO compacts sintered in loads air at 973K and 1123K and subjected to low applied uniaxial loads shown (in kg).
- Figure 3. Axial shrinkage versus radial shrinkage at 1123K for applied loads in kg.
- Figure 4. Creep strain versus time at 1123K for loads in kg.
- Figure 5. Relative density versus time at 1123K for loads in kg.
- Figure 6. Creep rate and densification rate versus stress at three relative densities.
- Figure 7. Scanning electron micrograph of a polished section of CdO sintered to a relative density,  $\rho$ , of 0.88.
- Figure 8. Axial shrinkage rate versus time for load change and constant load experiments.

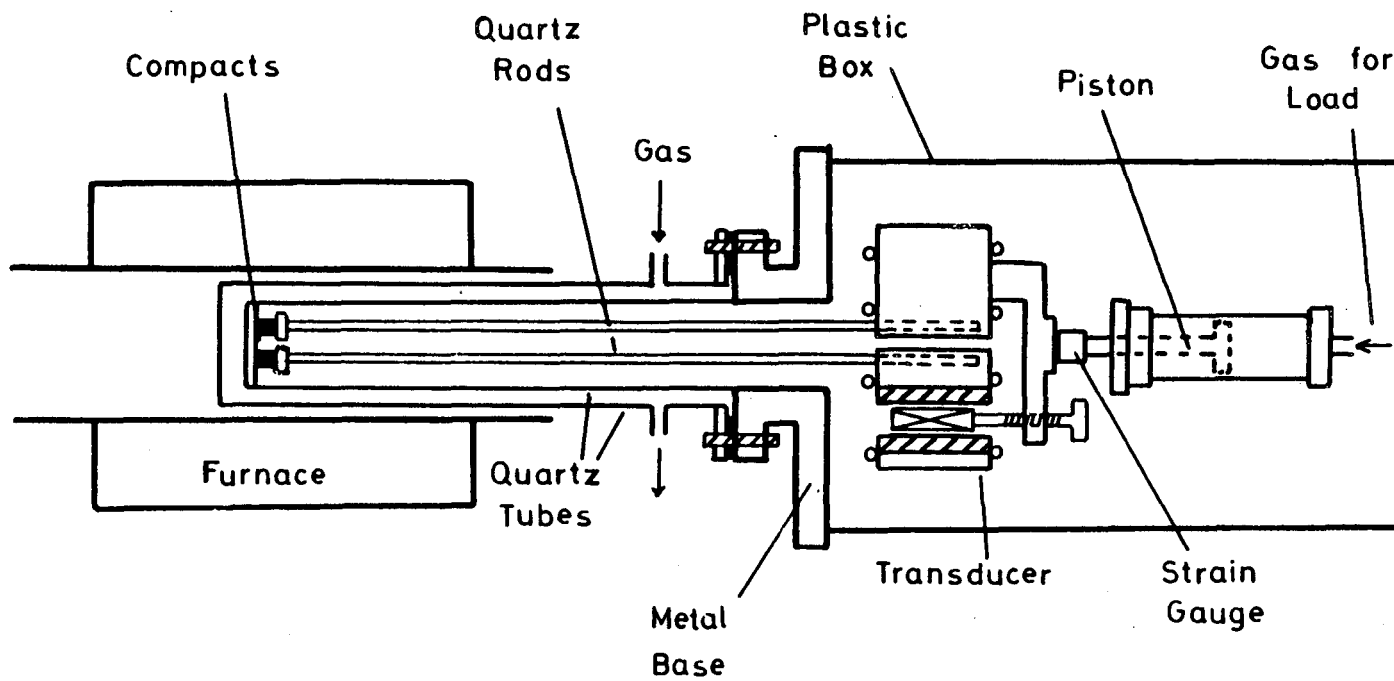
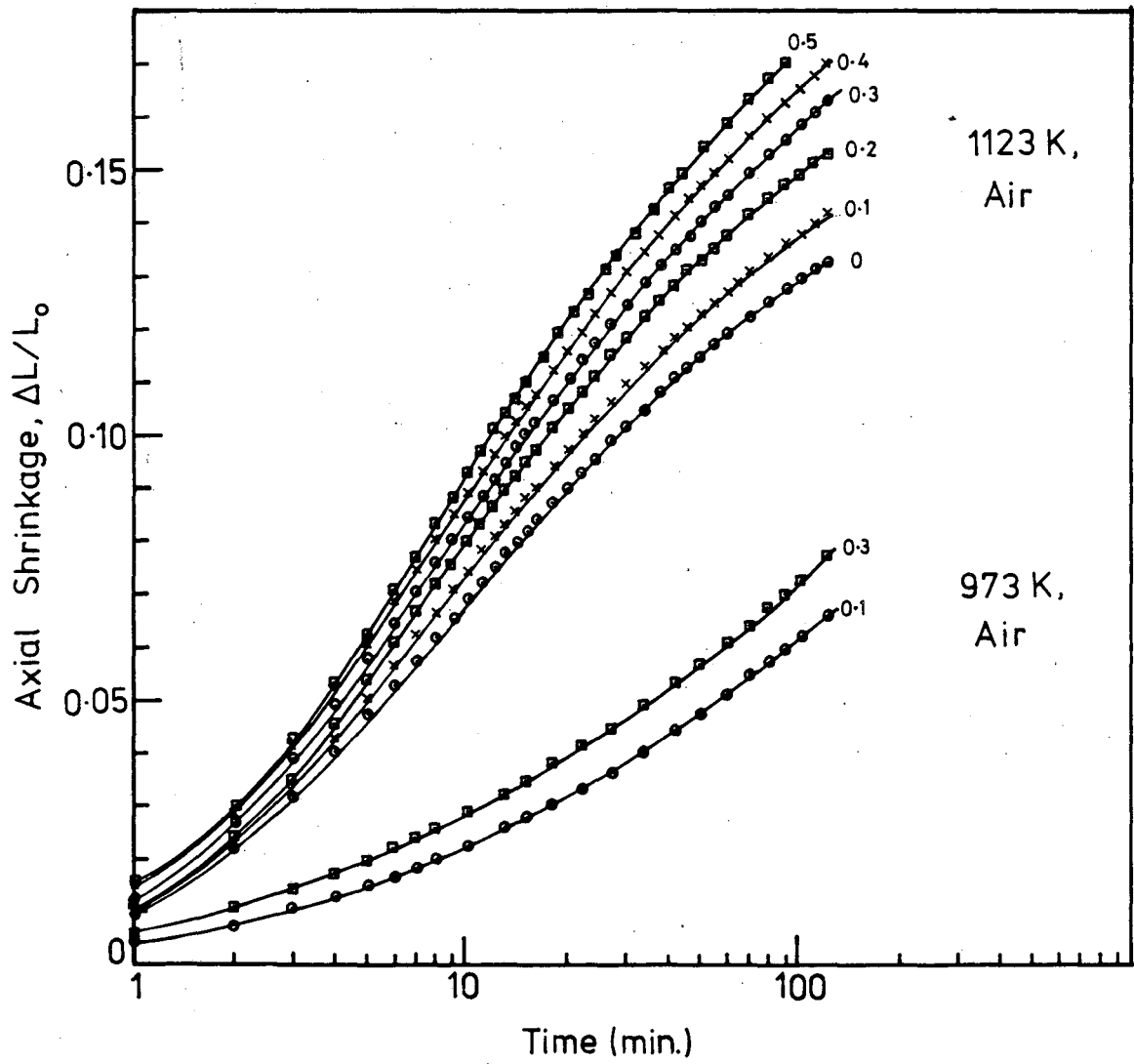


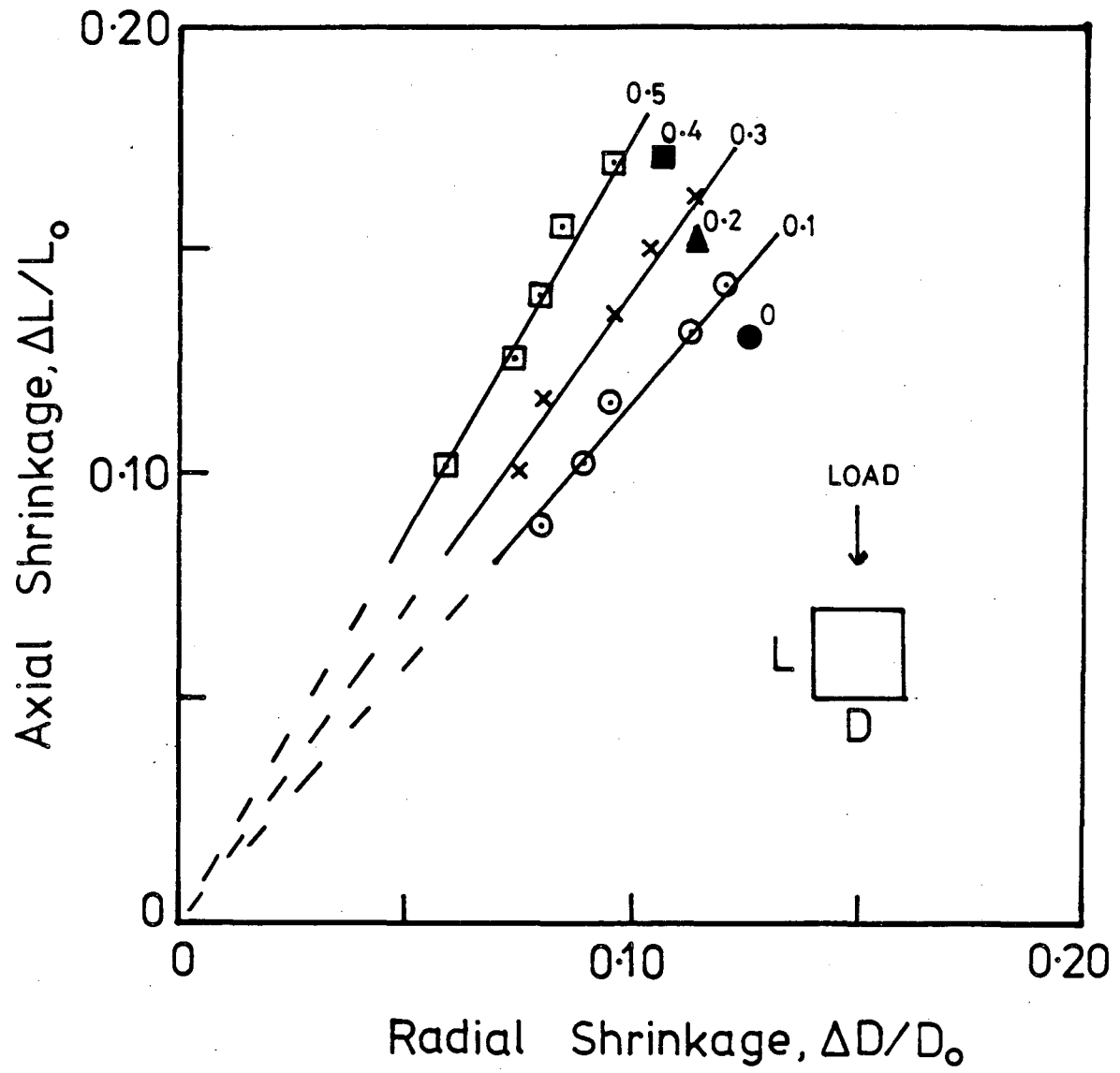
Fig. 1

XBL 847-2672



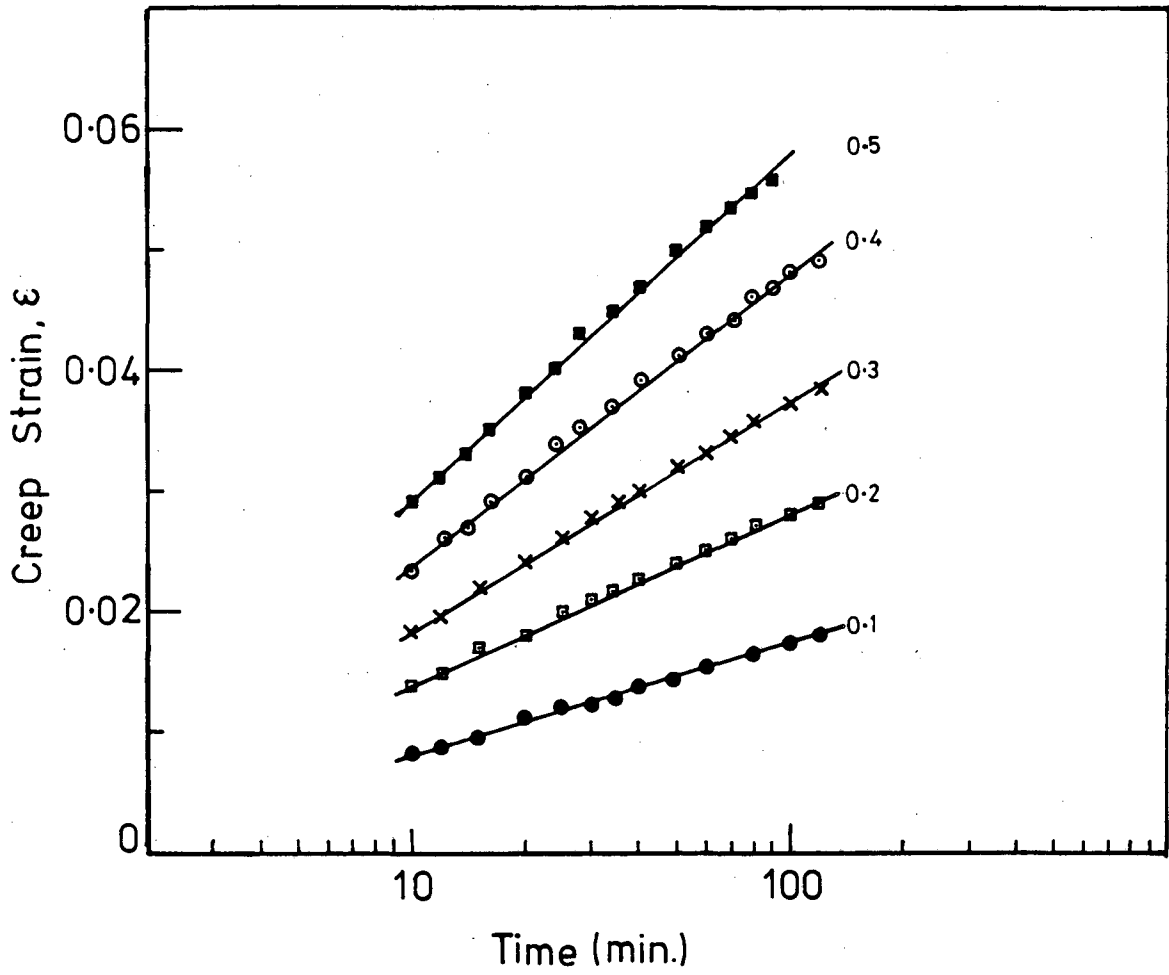
XBL 847-2673

Fig. 2



XBL 847-2674

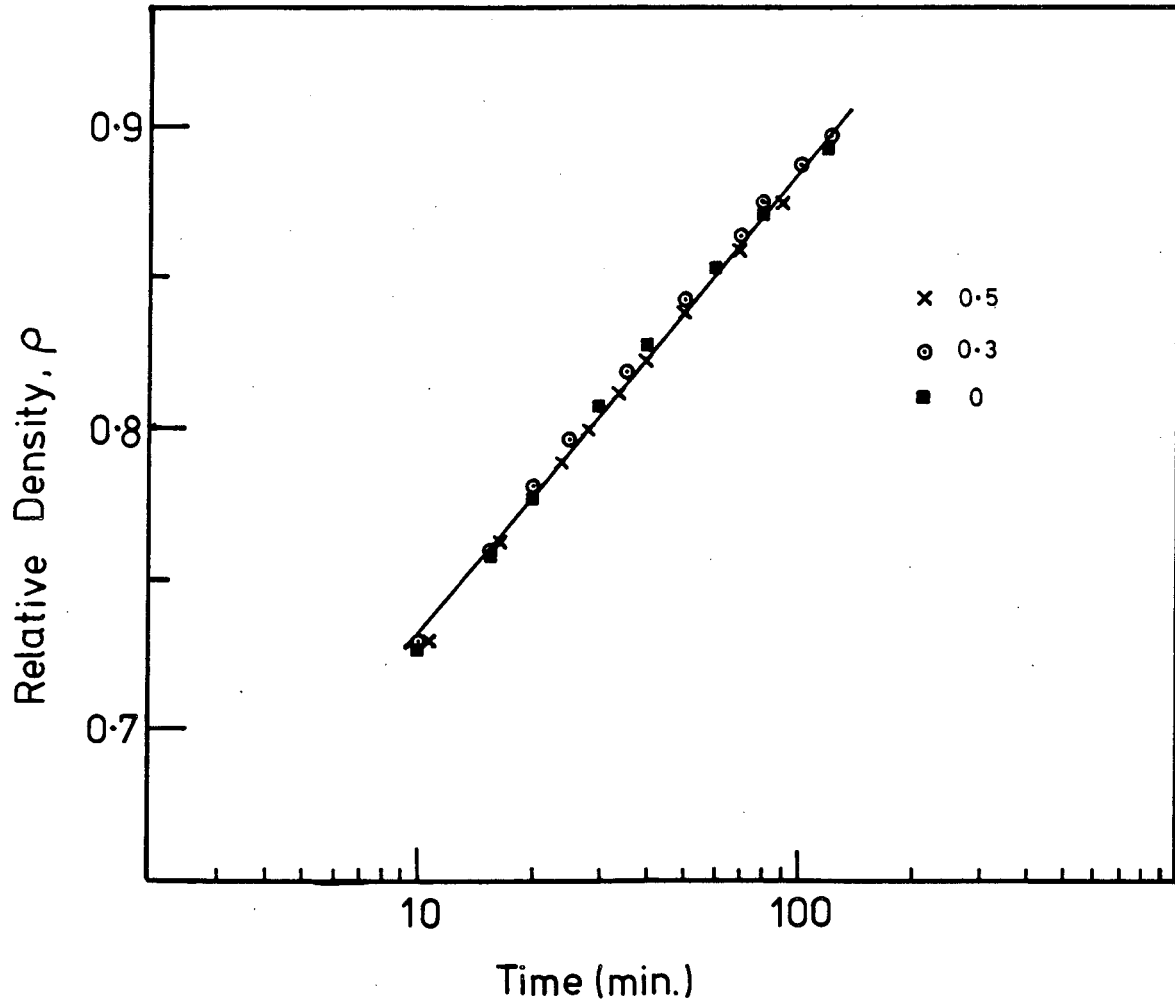
Fig. 3



XBL 847-2675

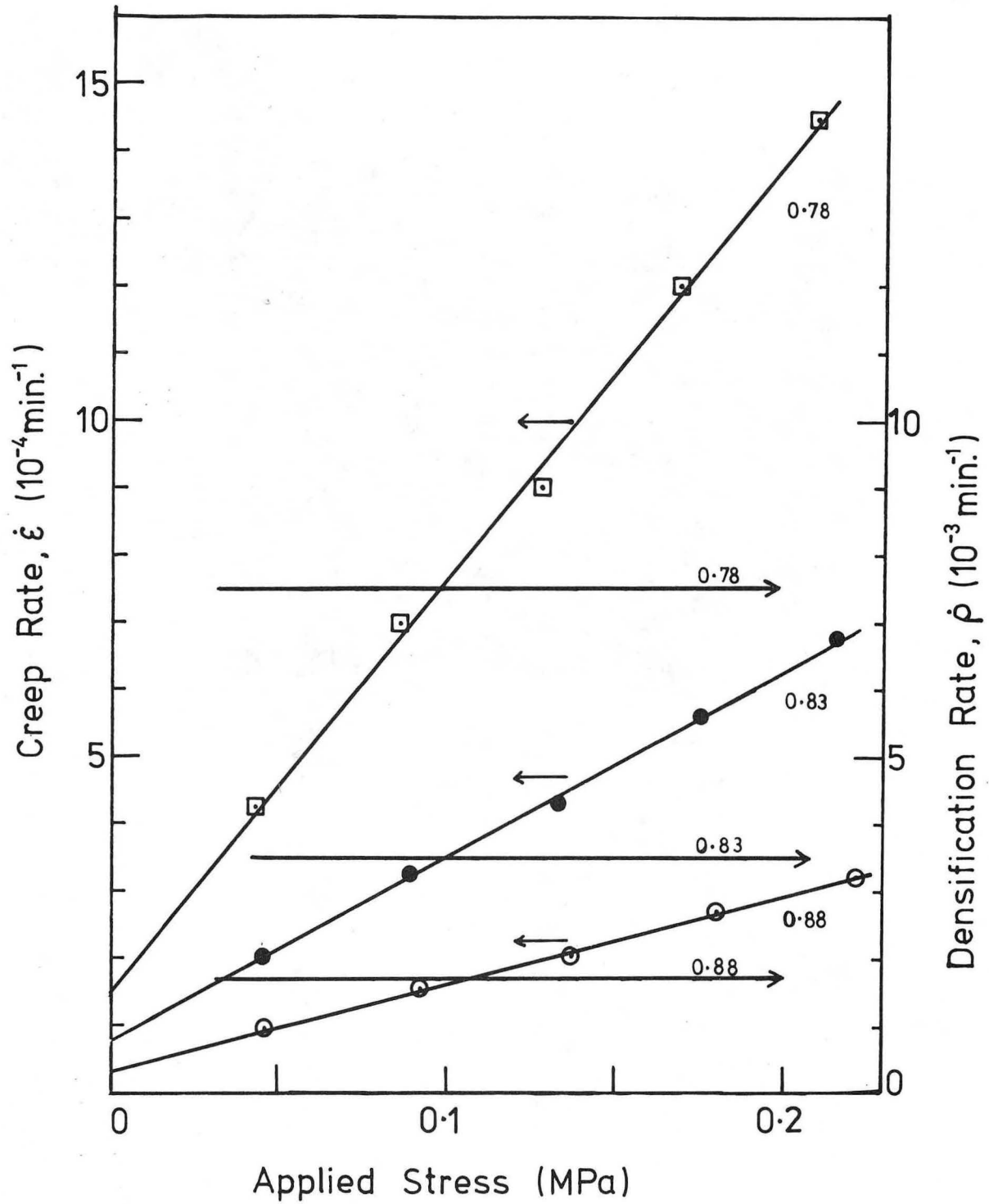
Fig. 4





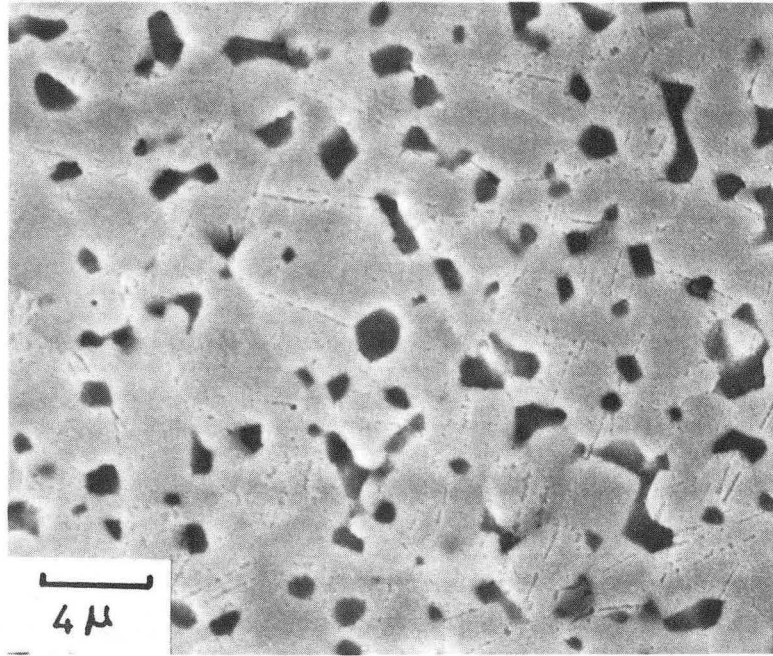
XBL 847-2676

Fig. 5



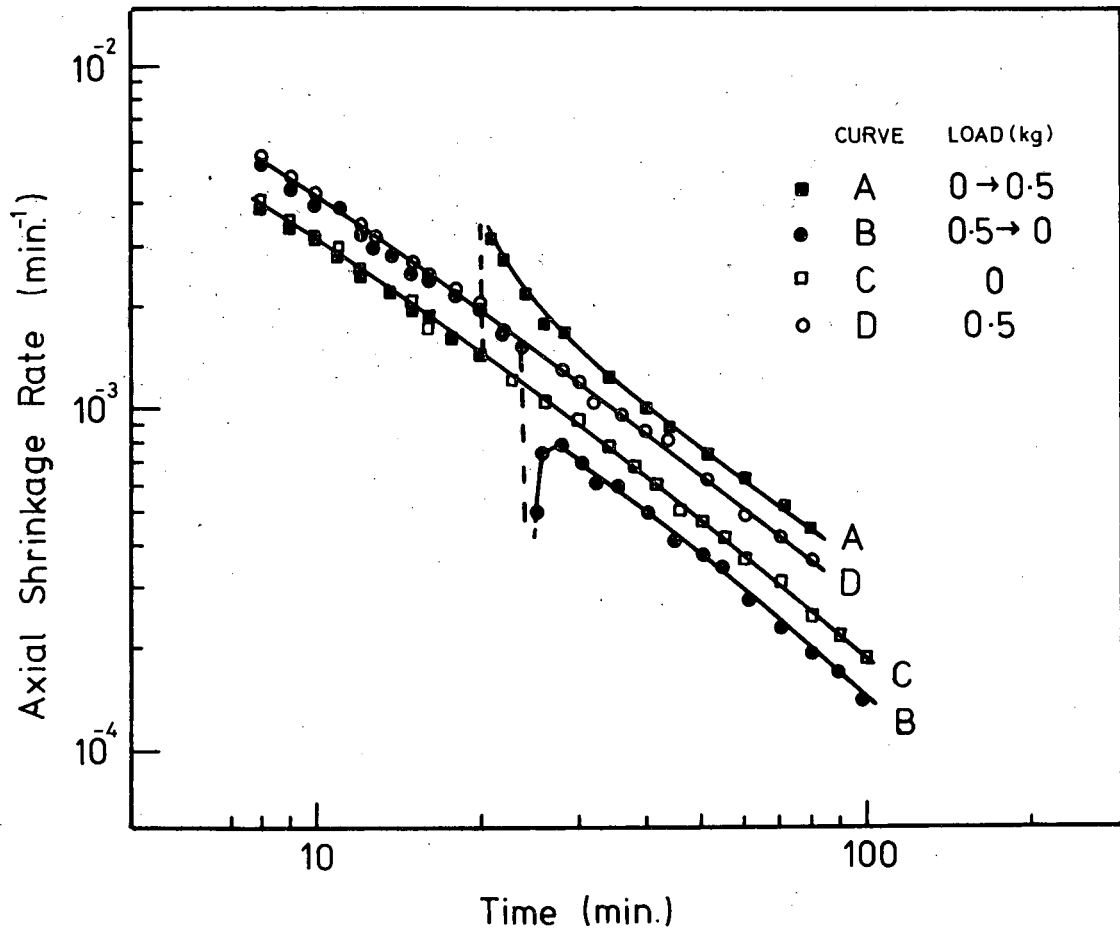
XBL 847-2677

Fig. 6



XBB 847-4869

Fig. 7



XBL 847-2678

Fig. 8

This report was done with support from the Department of Energy. Any conclusions or opinions expressed in this report represent solely those of the author(s) and not necessarily those of The Regents of the University of California, the Lawrence Berkeley Laboratory or the Department of Energy.

Reference to a company or product name does not imply approval or recommendation of the product by the University of California or the U.S. Department of Energy to the exclusion of others that may be suitable.

TECHNICAL INFORMATION DEPARTMENT  
LAWRENCE BERKELEY LABORATORY  
UNIVERSITY OF CALIFORNIA  
BERKELEY, CALIFORNIA 94720